

Supporting information

1. The energy dispersive X-ray pattern of ZnO/Au

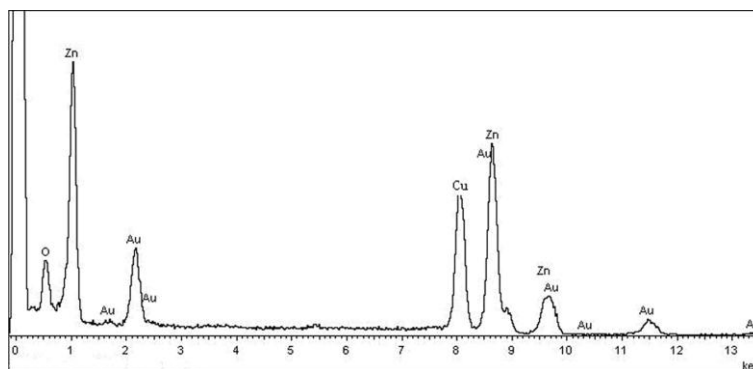


Figure S1. The energy dispersive X-ray pattern of ZnO nanorod decorated with Au nanoparticles

The energy dispersive X-ray pattern of ZnO nanorod decorated with Au nanoparticles in Figure S1 shows the Zn, O and Au elements, confirming the composition of both ZnO nanorods and Au nanoparticles.

2. The Raman characterization of Au/N719/dodecanethiol film

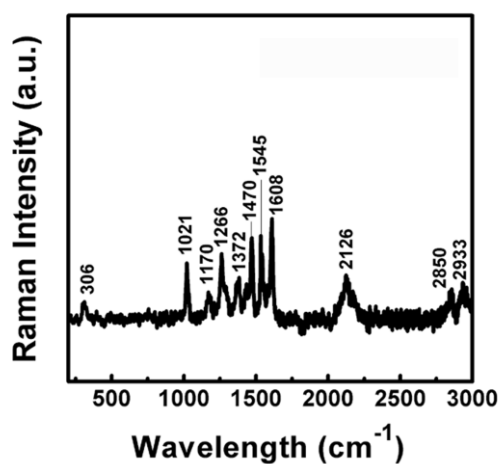


Figure S2. The Raman spectrum of Au/N719/dodecanethiol film

An Au/N719/dodecanethiol sample was fabricated to identify whether the Au-NCS banding can be replaced by Au-S banding during the dodecanethiol treatment. The Raman spectrum of Au/N719/dodecanethiol film (Figure S2) exhibits both N719 and dodecanethiol characteristics. N719 characteristics include benzene ring breathing (1021 cm^{-1}), C-C intern-ring (1266 cm^{-1}), symmetric COO^- stretch (1372 cm^{-1}), bipyridine bands ($1470, 1545, 1608\text{ cm}^{-1}$) and NCS band (2126 cm^{-1}). The dodecanethiol characteristics are the Raman vibrations of S-Au peak (306 cm^{-1}), C-C band (1170 cm^{-1}), CH_2 units (2850 cm^{-1}) and C-H band (2933 cm^{-1}), respectively. The Raman spectrum suggests the N719 molecules adsorbed on Au nanoparticle surface are not likely dissolved after the dodecanethiol treatment.

3. The dye loading amount on ZnO film and ZnO/Au film

Table S1. The dye loading amount on ZnO film and ZnO/Au film

Sample	ZnO	ZnO/Au
N719 loading amount (mol/cm^2)	1.41×10^{-7}	1.56×10^{-7}

The number of N719 dye molecules adsorbed on ZnO film and ZnO/Au film per square centimeter was calculated by measuring the absorbance of detached dye in basic NaOH solution (Table S1). The dye loading of ZnO/Au film is only 1.11 times larger than that in ZnO film.

4. The photocurrent density-voltage characteristics (J-V curves) of DSSCs with different photoanodes

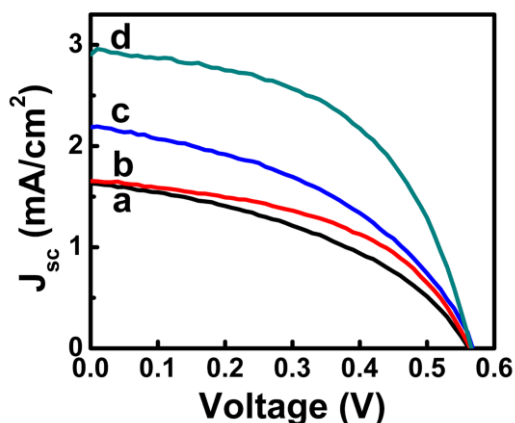


Figure S3. The photocurrent density-voltage characteristics (J-V curves) of DSSCs with ZnO/N719 (a), ZnO/N719/dodecanethiol (b), ZnO/Au/N719 (c) and ZnO/Au/N719/dodecanethiol (d) photoanodes.

Figure S3 shows the photocurrent density-voltage characteristics (J-V curves) of DSSCs with different photoanodes. Owing to the SPR effect of Au NPs, the current density (J_{sc}) of ZnO/Au/N719 device is increased by 29% (2.10 mA/cm^2) contrast to that of ZnO/N719 device (1.63 mA/cm^2), while the fill factor (FF) is almost unchanged, resulting in 0.54% in energy conversion efficiency. For the ZnO/Au/N719/dodecanethiol device, the dodecanethiol surface treatment on ZnO/Au/N719 photoanode increases the J_{sc} to 2.92 mA/cm^2 , while the FF is increase from 43 to 52, leading to 0.83% in energy conversion efficiency. The dodecanethiol adsorption on ZnO/Au/N719 photoanode may insulate vacant Au NPs sites as well as the exposed ZnO NRs sites. However the insulation on exposed ZnO NRs sites is not distinctive since the energy conversion efficiency only increase 0.05%, from 0.38% of ZnO/N719 device to 0.43% of ZnO/N719/dodecanethiol device. Hence, the insulation on vacant Au NPs sites is responsible for the significant improvement in ZnO/Au/N719/dodecanethiol device. Besides the energy conversion efficiency in ZnO/Au/N719/dodecanethiol device (0.83%) is more than twice of that of ZnO/N719 device (0.38%), consistent with the plasmon-enhanced absorption of ZnO/Au/N719/dodecanethiol film which is nearly twice as much as that of ZnO/N719 film. It indicates that the dodecanethiol treatment could fully exploit the

plasmon-enhancement absorption in DSSC.